



HAL
open science

Properties of cement pastes and mortars containing recycled green glass powder

Samir Nahi, Nordine Leklou, Abdelhafid Khelidj, Mohamed N Oudjit,
Abdelfatah Zenati

► **To cite this version:**

Samir Nahi, Nordine Leklou, Abdelhafid Khelidj, Mohamed N Oudjit, Abdelfatah Zenati. Properties of cement pastes and mortars containing recycled green glass powder. *Construction and Building Materials*, 2020, 262, pp.120875 -. 10.1016/j.conbuildmat.2020.120875 . hal-03492510

HAL Id: hal-03492510

<https://hal.science/hal-03492510>

Submitted on 26 Sep 2022

HAL is a multi-disciplinary open access archive for the deposit and dissemination of scientific research documents, whether they are published or not. The documents may come from teaching and research institutions in France or abroad, or from public or private research centers.

L'archive ouverte pluridisciplinaire **HAL**, est destinée au dépôt et à la diffusion de documents scientifiques de niveau recherche, publiés ou non, émanant des établissements d'enseignement et de recherche français ou étrangers, des laboratoires publics ou privés.



Distributed under a Creative Commons Attribution - NonCommercial 4.0 International License

29 between 7 and 90 days for mortar with glass powder, especially with 60% replacement showing
30 pozzolanic reaction taking place during this period. The pozzolanic reaction that occurs between glass
31 powder and calcium hydroxide ($\text{Ca}(\text{OH})_2$) to form more calcium silicate hydrate gel (C-S-H) leads to
32 the refinement of pores and the reduction of porosity.

33 **Key words:** glass powder, pozzolanic reaction, chemical shrinkage, porosity, dynamic Young's and
34 shear moduli.

35 **1. Introduction**

36 Glass is considered to be one of the most used materials in numerous quotidian applications. Glass can
37 be found primarily in the form of containers such as beer and soft drink bottles, wine and liquor
38 bottles, and bottles and jars for food, or in the flat form for windows and automotive industries. It can
39 also be found in cosmetics, appliances, electronics, fiber and other products. Ideally, waste glass
40 should either be reused or remanufactured to produce new glass products [1]. Though glass can
41 theoretically be completely recycled, there are still limitations in terms of meeting the quality criteria
42 for glass remanufacturing [2]. Just a small amount of the waste glass that is generated yearly is
43 recycled. Global recycling volumes in 2018 were estimated to be around 27 million tons, which
44 represents only 21% of the amount of glass produced [3]. A large amount is discarded and occupies
45 space in landfill or thrown and abandoned in nature. Its presence is not always aesthetically pleasing
46 and can represent a real danger to the safety of people and animals as well. Glass can cause serious
47 environmental pollution (air, soil and water pollution) because of being non-biodegradable. In addition
48 to landfill space, environmental and human constraints, glass is a non-renewable resource and its
49 recycling reduces non-renewable natural resource consumption, energy consumption and carbon
50 footprint.

51 Glass can be divided into several major families, depending on the field of application: soda lime,
52 borosilicate, aluminosilicate, lead glass, silica glass, zirconia glass, bio glass, fluorinated glass,
53 vitroc ceramic, chalcogenides, and metallic [4]. Among those families, soda-lime glass is the most
54 frequently used [4, 5] and the most investigated due to the large number of containers collected in

55 urban areas [6]. The particle size of glass has been found to have major impact on its usability in
56 concrete mixes [7]. Glass was first used as aggregate in cementitious material, but this attempt wasn't
57 successful due to the occurrence of alkali-silica reactions (ASR) [8].

58 Indeed, ASR can be mitigated by adding pozzolanic material such as fly ash [9, 10, 11], ground
59 granulated blast furnace slag [11, 12], silica fume [11], and even glass in powder form (GP) [11, 13,
60 14], or by adding steel fiber, lithium chloride or lithium carbonate compounds [11]. Conversely,
61 mortars with ground glass immersed in water for a period of seven years did not show any sign of
62 degradation due to ASR [15].

63 Finely ground glass is an amorphous material. When it is compared to other pozzolanic materials, we
64 can see that the overall content of SiO_2 , Al_2O_3 and Fe_2O_3 is similar or slightly lower than that of the
65 other mineral additions such as silica fume, fly ash or natural pozzolans [15, 16, 17].

66 Nowadays, ground glass pozzolans have been introduced as new supplementary cementitious
67 materials in Canadian standard A3018-18 [18]. The reactivity of glass powder is a compromise of
68 several parameters such as water-to-binder ratio, fineness, colors, temperature, etc. Much previous
69 work has been done in this field to understand the effect of particle size (or fineness), on glassy SCM
70 reactivity [1, 17, 19, 20, 21, 22, 23, 24]. Most of these tested glass powder below a certain grain size
71 or between two limited intervals of grain size so that it is difficult to assess the contribution of the
72 particle size on the Pozzolanic reactivity. This is due to a continuous gradation and flocculation of
73 particle size leading to difficulty of separation. In order to investigate the effects of particle size on
74 glass powder reactivity, Mirzahosseini et al. [19], prepared mortar and paste using glass powder with
75 very narrow particle size distributions 0-25 μm , 25-38 μm and 63-75 μm . Results indicate that mortar
76 with particle sizes in the range of 0-25 μm shows the highest compressive strength but that it is lower
77 than reference mortar even at 90 days. Patel et al. [20], studied the effect of glass powder particle size
78 decreases from 75 μm to 63 μm on mortar compressive strength. Results indicate that 20%
79 replacement of cement by GP with particle size smaller than 63 μm , gives compressive strength
80 comparable to reference mortar at 90 days and satisfies the Strength Activity Index (SAI) at 7 and 28
81 days. Whereas, in the case of particles smaller than 75 μm , just 10% to 15% of cement replacement by
82 GP can be used to reach satisfied SAI. Aliabdo et al. [21], found that the use of 10% glass powder

83 with particles size smaller than 75 μm as cement replacement enhances the mortar compressive
84 strength by about 9.0 % at 7 days. Parghi et al. [22], found that compressive strength of mortar made
85 with 5%, 10%, 15%, 20% and 25% glass powder having particle size smaller than 75 μm , as cement
86 replacement increases compared to the control mortar at 7, 28 and 90 days. Results done in this field
87 show that the pozzolanic properties of glass powder are highly influenced by the particle sizes of glass
88 or rather by its fineness of grinding and the amount of glass used. The reactivity and compressive
89 strength of cementitious materials increase as the particles size of the waste glass decreases and
90 fineness increases. According to Idir et al. [1], each kind of glass should be assessed in order to
91 evaluate its reactivity.

92 The optimum glass replacement partly depends on the particles sizes that govern pozzolanic reaction.
93 According to Du et al. [25], when using particles with mean diameters of about 3.4 μm , the optimum
94 GP replacement ratio in term of compressive strength is between 30% and 45%. Below the ratio of
95 30%, there is redundant portlandite in the cement hydration products, while when exceeding a ratio of
96 45%, insufficient portlandite is available for the GP pozzolanic reaction. Conversely, when it comes to
97 durability parameters such as chloride diffusion, water penetration depth and sorption, it is found that
98 concrete made with 60% GP shows better performance. According to Neithalalath et al. [26], the
99 incorporation of GP results in an increase of the hydration degree of the cement grains. The hydration
100 degree of glass powder depends partly on the cement substitution level. Increasing the GP content
101 decreases the calcium hydroxide content and leads to a decrease in the Ca/Si ratio, which becomes less
102 than 1 in the C-S-H formed due to less available Ca^{2+} and a lower pH in the pore solution. Thus, it will
103 weaken the hydration degree of the glass because of the instability and the easy decomposition of the
104 hydrates formed [5, 25].

105 Notwithstanding that the chemical composition of colored glass seems to be similar, there are great
106 differences in the structure depending on the role of each element as network former, modifier or
107 intermediate [4]. Among the divergent results found concerning the influence of glass particle
108 diameter on the reactivity of cementitious materials and the diversity of existing glass (type, colors),
109 just a few works, e.g. Du et al. [5, 25, 27], Liu et al. [28], have studied the influence of high glass
110 content (60%) on cement pastes, mortar and concrete characteristics. With high glass, the literature

111 does not show any results on chemical shrinkage of cement paste or dynamic Young's and shear
112 moduli of mortar. Additionally, there is limited available literature characterizing the microstructure of
113 mortar made with different rates of GP content taking into account their colors and particle size. In
114 order to bring more clarification to fresh and hardened characteristics especially concerning hydration,
115 microstructure and porosity further study is required. The purpose of this work is to investigate the
116 influence of cement replacement with soda lime Green Glass Powder (GR GP) on paste and mortar
117 characteristics. Increasing rates of GP replacement of cement by mass (10%, 25%, 35% and 60%) are
118 used. Material characteristics are evaluated by measuring flow, heat of hydration, chemical shrinkage,
119 compressive strength, and dynamic Young's and shear moduli, water evaporation and gives more
120 explanation about mortar microstructure and porosity. This study is done to determine the optimum
121 percentage of green glass powder and the possibility of high green glass usage.

122 **2. Materials and methods**

123 **2.1. Materials**

124 The main components of cement pastes and mortars used in this study are:

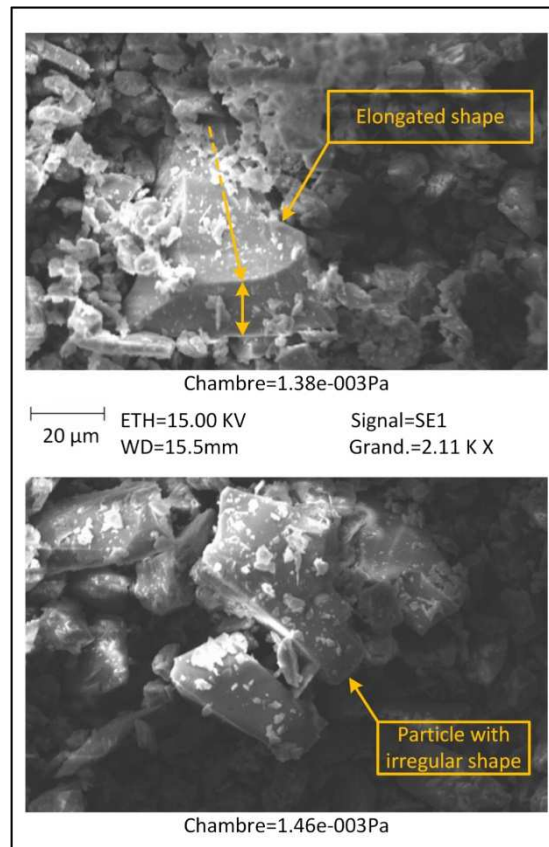
125 -Standard sand (0/2 mm), consisting of non-reactive siliceous rounded particles, conforming to
126 European Standard EN 196-1 [\[29\]](#).

127 -Ordinary Portland cement (OPC) CEM I 52.5 N which complies with European standard test EN 197-
128 1 [\[30\]](#).

129 -Green glass powder coming from various types of wine and liquor bottles collected from the seaside.

130 In order to study just the effect of glass as a SCM without the influence of contamination and
131 impurities caused by the different liquid content remaining in the bottles, plastic or paper labels stuck
132 on the bottle, and metal or plastic security rings, glass bottles are first cleaned and washed before
133 grinding. After that, they are dried and crushed. After removing plastic and metal impurities, they are
134 ground in a ball mill. The powder resulted is poured through a 0.063 mm sieve and the powder passing
135 through was used for this study.

136 According to a previous study [23], ground glass powder consists mainly of elongated and plate
137 shaped particles. Fig 1 Shows the surface texture of the finely ground GP using a scanning electron
138 microscope (SEM). As we can see from Fig. 1, glass consists of irregular and plate shaped particles
139 with smooth surface.

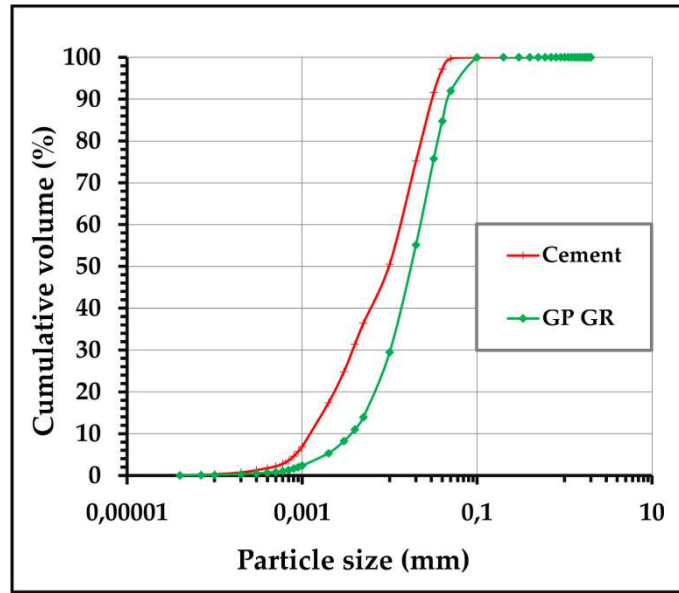


140

141

Fig. 1. SEM of green glass powder.

142 Particle size distribution of the cement and glass powder used for this work was determined by using a
143 laser particle size analyzer as shown in Fig. 2. Cement particles are finer than glass particles, the
144 average particle size for cement is 9.8 μm compared to 17.68 μm for glass.



145

146

Fig. 2. Particle size distribution of cement and glass powder.

147

The chemical composition of cement and glass powder are summarized in [Tab. 1](#).

Chemical composition (%)	OPC	GP
SiO ₂	20.07	73.64
Al ₂ O ₃	4.86	1.42
Fe ₂ O ₃	3.07	0.38
CaO	64.25	9.08
MgO	0.95	1.43
SO ₃	3.55	0.27
K ₂ O	1	0.01
Na ₂ O	0.18	11.62
P ₂ O ₅	-	0.01
TiO ₂	-	0.05
LOI	1.09	2.09

148

Table 1 Chemical composition of the cement and glass powder.

149

The cement bogue's composition and physical properties of the cement and glass powder are

150

summarized in [Tab.2](#).

151

152

153

Bogue's composition		
C ₃ S	60.8	
C ₂ S	14.6	
C ₃ A	8.2	
C ₄ AF	9.8	
Physical characteristics	OPC	GP
Specific gravity	3.16	2.5
Blaine (cm ² /g)	4290	3206
Particle size distribution (μm)		
Diameter at 10%	1.26	3.6
Diameter at 50%	9.80	17.68
Diameter at 90%	30.42	46.73

154 **Table 2** Cement Bogue's composition of and physical characteristics of cement and glass powder.

155 **2.2. Mix proportions and mixing procedure**

156 Cement paste and mortar mixes having the same binder composition, noted by 0 SCM, 10 GR GP, 25
157 GR GP, 35 GR GP and 60 GR GP, according to their cement replacement rates of 0%, 10%, 25%,
158 35% and 60% respectively, are prepared for this study (see [Tab. 3](#)). Followability, compressive and
159 flexural strength, water porosity, mercury intrusion porosimetry, mass variation, and dynamic Young's
160 and shear moduli tests are performed on simple mortar. Hydration heat assessment and chemical
161 shrinkage are evaluated for cement pastes. A water-to-binder ratio of 0.5 is used and kept constant for
162 all mixes used for tests except the chemical shrinkage mix, where a water-to-binder ratio of 0.4 is used
163 in order to avoid the risk of bleeding and its potential influence on chemical shrinkage. The mixing is
164 done according to the standard NF EN 196-1 [29]. Fresh pastes are directly tested after mixing for
165 chemical shrinkage and heat hydration assessment at 20 °C. Each mortar mix is composed of three
166 parts sand and one-part binder (cement and glass). For each mortar mixture, 40 × 40 × 160 mm
167 specimens are manufactured. After 24 hours (h) curing in a moist room at 20 °C and 90% relative
168 humidity (RH), the mortar bars are demolded and cured in a conditioned room at 20±2 °C. Specimens
169 designed for mechanical tests, water porosity and mercury intrusion porosimetry tests were
170 conditioned in water. Specimens for mass variation and dynamic Young and shear moduli tests are
171 conditioned in a climatic chamber at 50±5% RH.

Mix	0 SCM	10 GP GR	25 GP GR	35 GP GR	60 GP GR
Cement	100	90	75	65	40
Glass Powder	0	10	25	35	60

172 **Table 3** Binder composition of paste and mortar.

173 **2.3. Testing methods**

174 **2.3.1 Followability of mortar**

175 In order to access consistency for unconfined and consolidated fresh mortar made with different rates
176 of cement substitution by glass powder, a flow table test is performed according to EN 1015-3 [31]. A
177 standard conical mold, having an internal diameter of 100 mm at the base, 70 mm at the top and 60
178 mm height, provided with a riser, is used. Tests consist of 15 vertical shocks in 15 seconds to a mold
179 in which was placed a sample of fresh mortar. This latter is introduced on the mold in two layers, each
180 layer compacted with at least 10 strokes to insure uniform filling. After removing the mold, two
181 perpendicular spread diameters are measured and the flow diameter is expressed by the average.

182 **2.3.2 Heat evolution assessment**

183 Early age hydration kinetics of cement paste made with different levels of glass powder substitution
184 (0%, 10%, 25%, 35%, and 60%) is evaluated by using a TAM Air calorimeter device [32, 33]. Solid
185 raw materials are mixed in advance and then mixed with water for three minutes. Immediately after
186 mixing, samples of 4 to 6 g are taken and placed into standard plastic vials and then loaded into the
187 isothermal calorimeter. The heat release and heat flow results are normalized by the mass (g) of total
188 binder (cement + glass powder) and by mass of cement. The hydration heat measurement is continued
189 for approximately 96 h (4 days) under a constant temperature of 20 °C.

190 **2.3.3 Chemical shrinkage of cement pastes**

191 The chemical shrinkage of different cement pastes made with and without glass powder is measured
192 by gravimetric methods [34, 35]. Immediately after mixing, about 10 grams of mixed paste are placed
193 into a plastic cylindrical vial of about 2 cm in diameter and 5 cm in height. In order to ensure complete

194 percolation, a sample paste thickness of 7.0 mm to 8.0 mm is used. Water is added drop by drop to
195 minimize the disturbance of the paste top layer. Cement paste is introduced into the vial without
196 trapping of air bubbles in the paste. The vial is hung on a balance (accuracy 0.0001 g) by a nylon
197 thread and immersed in a water bath at 20 °C.

198 Tests start 30 minutes after initial water-cement contact for all cement pastes and last 48 h. The
199 apparent mass of the vial with cement paste is recorded automatically every 5 minutes. The hydration
200 process lead to volume changes of the cement paste. Water penetrate into the paste and fill the
201 porosities generated by Le Chatelier's contraction. Chemical shrinkage of cement paste $CS(t, T)$
202 (mm^3/g of initial anhydrous cement) is calculated as follows:

$$203 \quad CS(t, T) = \frac{MS(t) - MS(t_i)}{MC \cdot \rho_w(T)} \quad \text{Eq. (1)}$$

204 where $MS(t)$ is the apparent mass of both the vial and the sample as recorded by the balance at time t
205 (g); $MS(t_i)$ is the apparent mass of both the vial and the sample at initial time t_i (g); $\rho_w(T)$ is the water
206 density (g/mm^3); T is the water bath temperature ($^{\circ}\text{C}$); MC is initial anhydrous cement mass of the
207 sample (g).

208 **2.3.4 Compressive and flexural strength of mortar**

209 The compressive and flexural strength tests were conducted according to EN 196-1 [29] at 7, 28 and
210 90 days using $40 \times 40 \times 160 \text{ mm}^3$ cubes. Three flexural strength tests and six compressive strength
211 tests were conducted for each mix, where the average and the standard deviation were reported.

212 **2.3.5 Mercury intrusion porosimetry of mortar**

213 In order to investigate the pore network of the mortars, a classical mercury intrusion porosimetry
214 (MIP) technique was used. It is based on the premise that when a nonwetting fluid (one having a
215 contact angle greater than 90° : mercury) is forced into the pores of the sample by increasing pressure,
216 the higher the pressure, the smaller the pore that the fluid can enter. The relationship between the
217 pressure and capillary diameter is described by Washburn's equation as follows:

$$218 \quad d = \frac{-4 \gamma \sin \phi}{p} \quad \text{Eq. (2)}$$

219 Where d is the size of an equivalent cylindrical pore that requires a given pressure p to be filled, γ is
220 the surface tension of the mercury, and θ is the contact angle between the mercury and the pore wall.
221 The values for γ and θ are assumed to be 0.485 N/m and 130° , respectively.

222 Mercury porosimetry is an extremely useful characterization technique for porous materials [36]. It is
223 a widely recognized technique for characterizing the distribution of pore sizes in cement-based
224 materials [37].

225 MIP tests are carried out on specimens with an apparent volume of about 3 cm^3 , cut from the core of
226 the mortar cube after 28 and 90 days of curing. In order to make the small specimens devoid of
227 moisture, they are dried in an oven at 40°C until the mass stabilized. The dried specimens are kept in
228 the oven until the start of the test. The pressure range used was from sub-ambient up to 375 MPa,
229 covering a pore diameter ranges from about $200 \mu\text{m}$ to 3 nm.

230 **2.3.6 Dynamic Young's modulus, dynamic shear modulus of mortar**

231 Dynamic Young's modulus and dynamic shear modulus of the mortar specimens are measured using a
232 Grindosonic apparatus following ASTM E 1876-01[38] and NF EN ISO 12680-1[39]. Tests are
233 performed on prismatic specimens with standard dimensions of $40 \times 40 \times 160 \text{ mm}^3$. The test is based
234 on exciting vibrations in the mortar prism by striking them with a small tapping device. A vibration
235 sensor detects the flexural or torsional vibrations, which are then analyzed by the Grindosonic device.
236 The resonant frequency is manually recorded from data acquisition related to excitation system.
237 Elastic dynamic modulus is determined from the density and resonant frequency of the mortar. For
238 each mixture, dynamic Young's and shear moduli tests are performed on three specimens and the
239 average is reported. Specimen mass is recorded for each specimen as well.

240 **2.3.7 Water porosity of mortars**

241 Water porosity testing consists of measuring the percentage of voids that are connected to the surface
242 of hardened mortar and accessible by water. Tests are carried out using the French standard NF P 18-
243 459 [40], modified by adding new steps consisting of half immersing the sample in water for 24 h
244 under vacuum pressure to ensure complete saturation of the specimens after total immersion. Water
245 porosity tests are carried out on three prismatic specimens at 7, 28 and 90 days. Samples are first put

246 under the vacuum pressures until reaching a pressure of 25 milibar. This vacuum is maintained for 4 h.
 247 After that, the specimens are half submerged in water for 24 h under pressure followed by total
 248 immersion in water for 48 h to suck water into the small pores. The porosity is obtained by weighing
 249 the specimen in water and saturated surface-dried. The same specimen is dried in an oven at 105 °C
 250 until constant mass. The water porosity is calculated as follows:

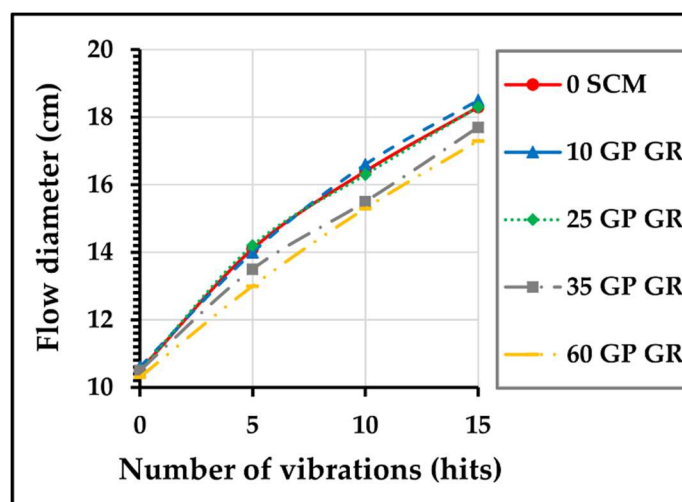
$$251 \quad n = \frac{M_{air} - M_{dry}}{M_{air} - M_w} \quad \text{Eq. (3)}$$

252 Here M_{air} is mass of the mortar specimen at the saturated surface-dried state, M_{dry} is the mass of mortar
 253 specimen at oven dried state, and M_w is the mass of mortar specimen saturated in water.

254 3. Results and discussions

255 3.1. Mortar Flowability

256 Fig.3. shows the flows of mortars made with different amounts of glass powder. It can be seen from
 257 this figure that there is no variation in the flow of mortar made with 10% and 25% replacement of
 258 cement by glass powder compared to the reference mortar in both vibrated or non-vibrated form (0
 259 hits). However, a slight decrease in the flow is seen with mortar made with 35% and 60% replacement
 260 in vibrated form contrary to non-vibrated form, which remains the same as the reference. The increase
 261 of glass powder replacement from 35% to 60% decreases the flow value.



262

263

Fig. 3. Flowability of mortar made with different amounts of glass powder.

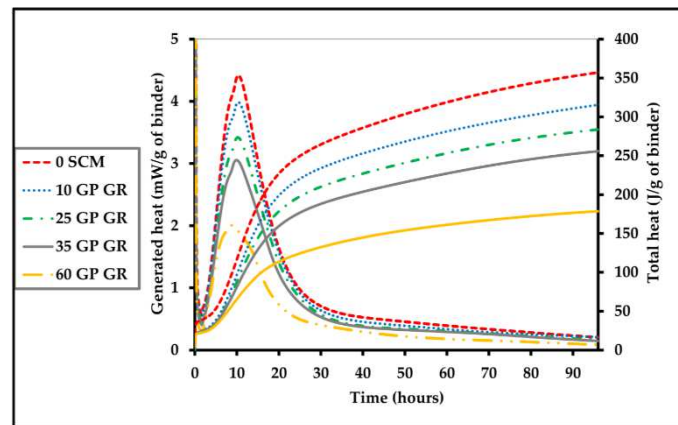
264 A previous study by Sadiqul Islam et al. [41], shows that a minor increase in flow mortar is achieved
265 with an increase of glass powder replacement (10%, 15%, 20%, and 25%); they reported that this
266 increase might result from the effect of glass material, which is cleaner in nature. According to Taha et
267 al. [42], when using glass powder with particles size below 45 μm , the slump value of concrete is not
268 affected by 20% replacement. Schwarz et al. [43] evaluated the workability of plain cement and
269 cement replaced with glass powder at rates of 10%, 20%, and 30% by mass. Results indicate that
270 increasing glass powder content leads to increased flow due to the nonabsorbent nature of glass
271 increasing free water content. Aliabdo et al. [21] found that the use of glass powder as cement
272 replacement (5%, 10%, 15%, 20%, and 25%) increases concrete slump. This behaviour may be due to
273 the glassy surface and low water absorption of glass powder or may be attributed to the coarser
274 particles of glass powder compared with cement. In contrast, the same authors [21] reported that the
275 use of glass powder as cement addition (5%, 10%, 15%, 20%, and 25%), which increase the binder
276 amount (cement and glass powder) compared to the amount of binder in the case of using glass
277 powder as cement replacement, decreases concrete slump. This trend may be due to the increase of
278 fine material content which increases the cohesion of concrete mix and thus decreases the concrete
279 slump. Lu et al. [44] studied the effect of 20% replacement of cement by GP with different particles
280 sizes (204 μm , 88.5 μm , 47.9 μm , 28.3 μm and 18.8 μm). Results indicate that bigger particle size and
281 irregular shape of glass particles hinder the movement of fresh mortar and result in a reduction of
282 flow. Liu et al. [28] prepared mortar with a low water-to-binder ratio (0.25) and the same dosage of
283 super plasticizer, using increasing content of glass powder as cement replacement (10%, 30% and
284 60%). They reported that the flowability of mortar increases with increasing glass content. However,
285 when preparing the same mixtures with a high water-to-binder ratio (0.5) and without super
286 plasticizer, results show no significant change on the flowability or even a slight decrease with high
287 volume recycled waste glass content.

288 Based on the literature and our results, there are contradictory results about the influence of GP as
289 cement replacement on the flowability of cementitious materials. This can be explained by
290 counteracting effects of several parameters such as the shapes of particles, their size, the nonabsorbent
291 nature of glass, the smooth surface of glass particles, the influence of particle wettability and the

292 amount of cement replacement. Irregularly shaped particles with high aspect ratios and sharp edges
 293 decrease fluidity. However, due to the grinding effect, the shape of the particles is more favorable to
 294 fluidity. The non-absorbent nature of glass particles increases the effective water to cement (w/c) ratio
 295 and enhances the flowability. Small particles need more water to wet their surface. Smooth surfaces
 296 promote particle movement; this increases fluidity. The rate of replacement is an important parameter
 297 since the increased amount of glass leads to an increase of water in the mix. Moreover, there is not
 298 much cement paste in the mix, which can decrease the particle's friction and increase the fluidity.

299 3.2. Heat of hydration assessment

300 The heat rate and the total achieved heat of cement pastes containing GP under a constant temperature
 301 of 20 °C over 96 h, normalized by the amount of binder and the reference cement paste are shown in
 302 Fig. 4. Their peaks' age and intensity hydration value are presented in Tab. 4. The relative values of
 303 the principal heat rate peaks of 10 GR GP, 25 GR GP, 35 GR GP and 60 GR GP pastes to the principal
 304 heat rate peak value of reference cement paste 0 SCM were found to be 0.903, 0.774, 0.692, 0.455
 305 respectively.



306
 307 **Fig. 4.** Hydration heat assessment of glass powder blended cement pastes, normalized by the amount
 308 of binder (cement and glass powder).

Mixture	Age of hydration peaks		Intensity of hydration peaks	
	Measured Value (hours)	Value relative to reference paste (%)	Measured Value (hours)	Value relative to reference paste (%)
0 SCM	10.37	100	4.42	100
10 GP GR	10.34	99.7	3.99	90.3
25 GP GR	10.22	98.6	3.42	77.4
35 GP GR	9.91	95.6	3.05	69.2

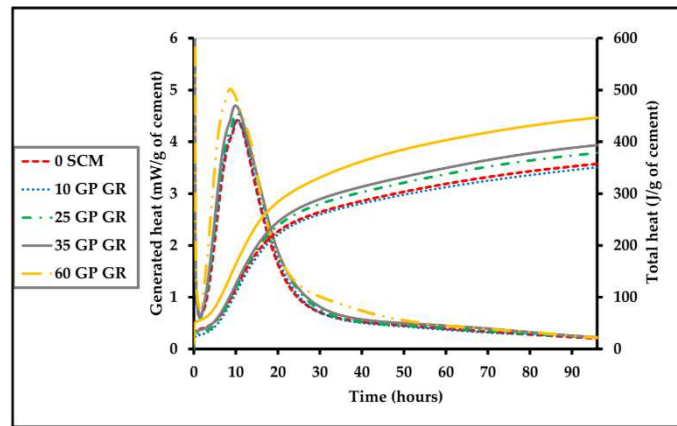
60 GP GR	8.65	83.4	2.01	45.5
----------	------	------	------	------

309 **Table 4** Characteristic values of isothermal calorimeter tests.

310 The relative values indicate that the replacement of cement by GR GP caused a reduction in the heat
311 rate. This result is in accordance with previous literature [28, 44]; they reported that the rates of heat
312 evolution of the waste GP modified pastes are lower than that of the pure cement pastes. This
313 demonstrates that the waste GP has a lower reactivity at the early stages of hydration. It is important to
314 note that the heat rate of paste with 60% replacement by GP is less than the half that of the reference.

315 The principal peaks of hydration for cement pastes containing glass powder occur earlier than that of
316 cement paste without glass powder, 0 SCM. The relative times of the apparition of the peaks heat rates
317 of 10 GR GP, 25 GR GP, 35 GR GP and 60 GR GP pastes to the time of the peak heat rate for the
318 reference cement paste 0 SCM are found to be 0.997, 0.986, 0.958, 0.834. This indicate that the time
319 to reach the first heat flow peak decreases with the increase of glass powder content. This acceleration
320 of the hydration process of cement can be explained by the increase of the effective water to cement
321 (w/c) ratio due to the replacement of cement by glass powder and the high alkali content of glass
322 powder. Huang et al. [45], reported that the alkali in cement accelerates the hydration at early ages.
323 High alkali addition of cement shortens the induction period and promotes the dissolution of C_3S and
324 the formation of $Ca(OH)_2$. According to Du et al. [27], fine glass powder can accelerate hydration via
325 the adsorption of calcium ions from the liquid phase and acts as nucleation and growth sites for C-S-H
326 and other hydrates. Moreover, the higher content of alkalis (Na_2O) may act as catalysts in the
327 formation and growth of C-S-H at an early age [46, 47].

328 When calorimetry results are expressed as the heat evolution normalized to the cement component as
329 shown in Fig. 5, we can see that the replacement of recycled waste glass increases the reaction rate for
330 all paste made with glass powder except the 10 GP GR paste, which remains the same. The reaction of
331 the cement component is enhanced due to the physical presence of glass powder. This so-called filler
332 effect is attributed to two main factors: the available space for the hydrates of the clinker phases to
333 form in and the surfaces grains, which act as sites for the heterogeneous precipitation and growth of
334 hydrates [48].

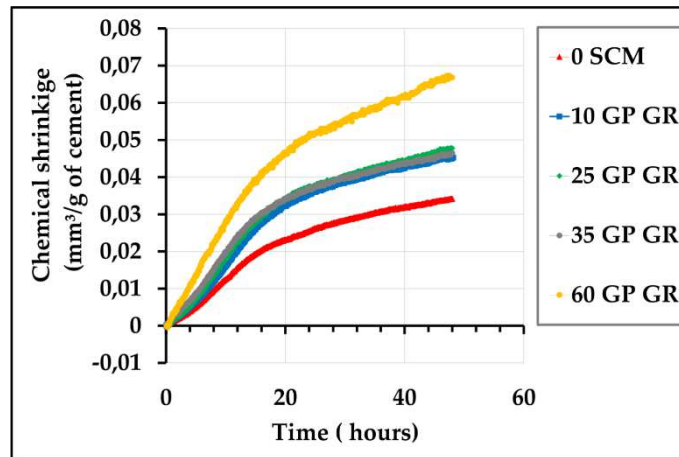


335

336 **Fig. 5.** Hydration heat assessment of glass powder blended cement pastes, normalized to the cement
 337 component.

338 **3.3. Chemical shrinkage**

339 **Fig. 6** shows chemical shrinkage test results over 48 h, normalized by cement mass, of the control
 340 paste and pastes modified with 10%, 25%, 35% and 60% glass powder. It is clear from this figure that
 341 chemical shrinkage, normalized by cement mass, for all cement paste samples increases throughout the
 342 hydration process. Chemical shrinkage is related to the volume change during the time. The volume of
 343 the resulting hydrates during the hydration process is lower than that of the initial reactants (cement,
 344 glass powder and water) [34]. It is also seen from **Fig. 6** that increased glass powder in cement paste
 345 increases the normalized chemical shrinkage, especially with 60% cement replacement with GP,
 346 where cement contains high amounts of C_3A and glass powder has high alkali content (Na_2O).
 347 According to Yodsudjai. [49], the chemical shrinkage of paste increases with the C_3A and C_4AF
 348 content and equivalent alkali content. Moreover, increasing glass powder content causes more
 349 available water for the hydration of cement particles, which is expected to increase chemical
 350 shrinkage.



351

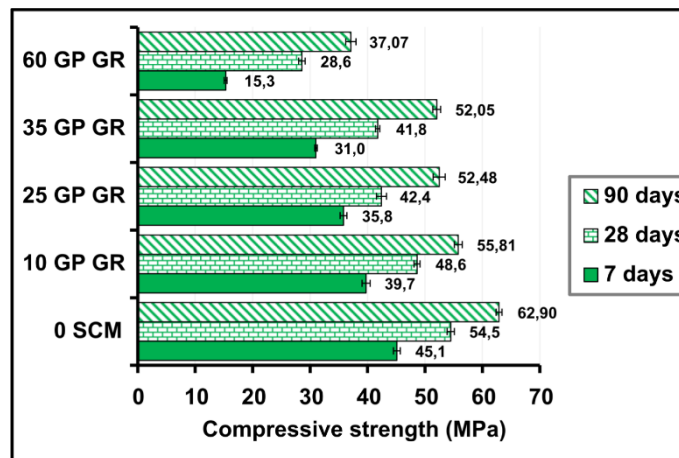
352

Fig. 6. Evolution of chemical shrinkage versus time for cement pastes with different glass powder contents (w/b = 0.4).

353

354 3.4. Compressive and flexural strength:

355 Fig.7 and Fig.8 show the compressive and flexural strength variation of cement mortar samples with
 356 and without glass powder after 7, 28 and 90 days of moist curing.



357

Fig. 7. Effect of GP replacement ratio on the compressive strength of mortar at 7, 28 and 90 days.

359

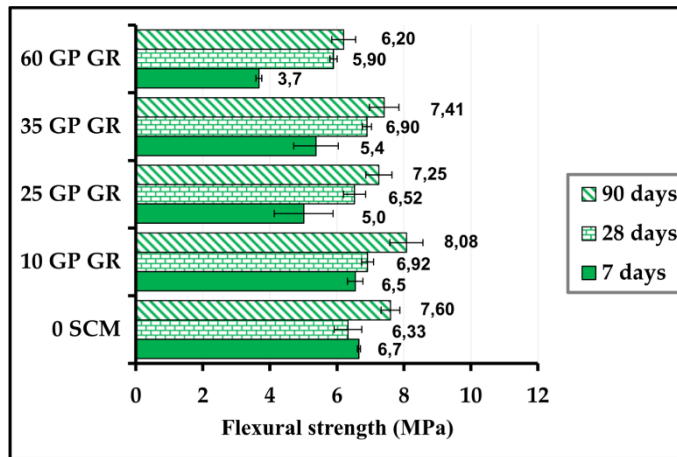


Fig. 8. Effect of GP replacement ratio on the flexural strength of mortar at 7, 28 and 90 days.

360

361

362

363

364

365

366

367

368

369

370

371

372

373

374

375

376

377

378

379

From these figures, it is clear that the compressive and flexural strength of cement mortar specimens increase with age. Increasing the glass powder amount as cement replacement decreases the compressive strength at all curing periods in this study. In general, flexural strength follows the same trend as compressive strength, low difference is noticed for all mortars made with glass powder compared to the reference. Higher reduction in compressive strength is seen at an early age than at the latest age, which is in accordance with previous findings [25]. The lowest value is obtained at 60% GP GR. A substantial difference is observed between the control mix 0 SCM and the 60 GP GR mix at 7 days. The reduction in the strength values at the early age can be explained by the reduction of the amount of clinker compounds responsible for strength development at early age. The compressive strength hardly changes throughout the 90-days period for mortar with 60% of glass powder. This can be explained by the long-term activity of pozzolanic reactions. With longer curing, the amorphous silica in glass powder slowly dissolves under the alkaline environment and reacts to form $\text{Ca}(\text{OH})_2$ in the pore solution C-S-H gels [5, 25].

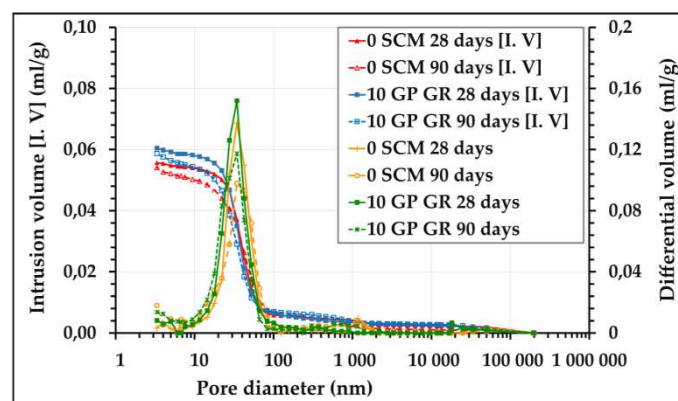
At 90 days, the compressive strength is very similar for mortar with 25% and 35% glass powder substitution. This may be due to the pouzzonanic activity of the additional glass powder (10% by weigh of cement) from 25% to 35% that still shows pozzolanic activity. Enough late strength is provided to compensate for the lower early strength. These results can be emphasized by the slow rate

380 of glass powder pozzolanic reaction since the compressive strength at 7 days is greater for mortar with
381 25% cement substitution by glass powder that in mortar with 35% replacement.

382 Using a water-to-binder ratio of 0.487, Du et al. [25] studied the effect of compressive strength on
383 concrete made with GP as cement replacement at 15%, 30%, 45 %, and 60% by weight of the total
384 cementitious materials. The mean diameter of the glass particles is 3.4 μm . Results indicate that with a
385 longer curing age (28 and 90 days), the compressive strength continuously increases with GP
386 replacement level up to 45%, and the concrete mixture with 60% GP exhibits a comparable strength to
387 the reference mixture. Two main factors could explain the contradictory results found on concrete
388 compared to the current results for mortar compressive strength: the interfacial transition zone between
389 cement paste and aggregate on concrete, which is more densified using glass powder, and the particle
390 size used, that is 3.4 μm compared to the 17.68 μm mean diameter in the present work.

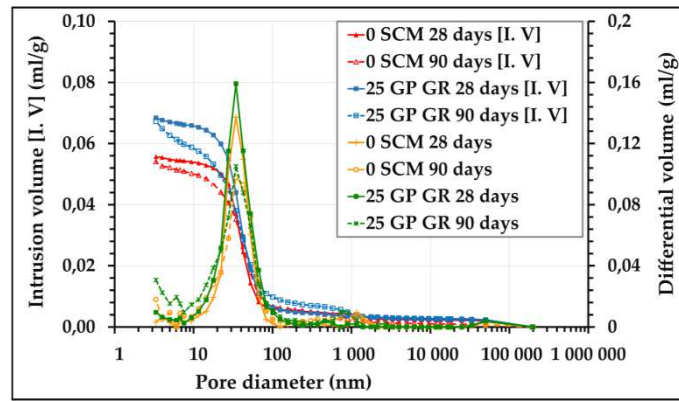
391 3.5. Mercury intrusion porosimetry

392 In this section, the pore structure results of mortar made with cement substituted with glass powder at
393 0%, 10%, 25%, 35%, and 60% after 28 and 90 days' curing are discussed. The cumulative intrusion
394 versus pore diameter curves and differential curves are shown in Fig. 9.A, Fig. 9.B, Fig. 9.C, Fig. 9.D
395 and Fig. 9.E.



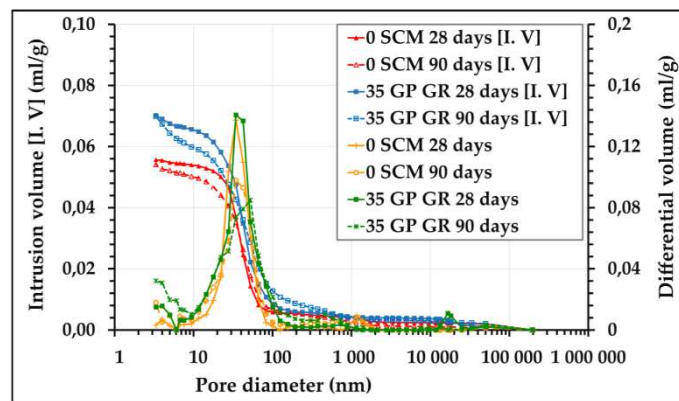
396
397 **Fig. 9.A.** Cumulative and differential pore size distribution of mortar made with 10% glass powder at
398 28 and 90 days.

399



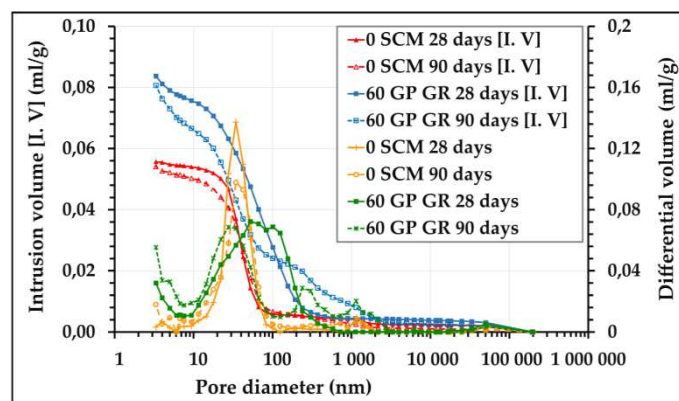
400 **Fig. 9.B.** Cumulative and differential pore size distribution of mortar made with 25% glass powder at
401 28 and 90 days.

402

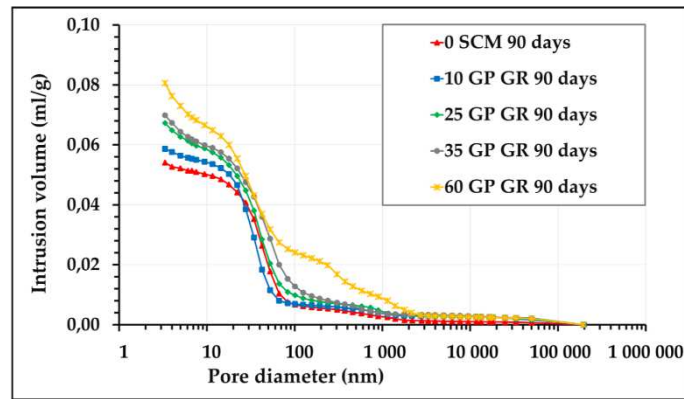


403 **Fig. 9.C.** Cumulative and differential pore size distribution of mortar made with 35% glass powder at
404 28 and 90 days.

405



406 **Fig. 9.D.** Cumulative and differential pore size distribution of mortar made with 60% glass powder at
407 28 and 90 days.



408

409 **Fig. 9.E.** Cumulative pore size distribution of mortar made without and with different glass powder
 410 content at 90 days.

411 We can see from these figures that the pore size distribution is affected by the glass powder rate
 412 substitution. The mortar containing glass powder shows higher porosity than the reference at 28 and
 413 90 days. The highest value is obtained with 60% replacement. This finding supports the compressive
 414 strength results, which are low.

415 The main peak intensity increases with 10% and 25% replacement of cement by glass powder at 28
 416 and 90 days. Mortar with 35% replacement of cement by glass powder shows the same peak intensity
 417 as reference mortar at 28 days. In contrast, at 90 days, the main peak intensity decreases compared to
 418 the reference. The same trend is shown with 60% replacement of cement by glass powder. The main
 419 peaks denote remarkable decreases compared to the reference whether at 28 or 90 days. The main peak
 420 is also shifted towards bigger pores at 28 days. At 90 days it moves towards smaller pores; at the same
 421 time new peaks with small intensities reflecting bigger pores are created. This can be explained by the
 422 dilution effect of cement, which leads to much more available space reflecting that higher porosity and
 423 the hydration process and pozzolanic reaction that lead to the densification and the refinement of the
 424 microstructure. Results of the same nature were found by Liu et al. [28] while studying the
 425 microstructure of normal strength sample mortar containing 60% mixed colored waste glass. They
 426 associated the higher porosity to the lower gel-to-space ratio, which is caused by the higher water-to-
 427 binder ratio.

428 Another important parameter that should be taken into consideration to explain the porosity increase,
 429 is the increased volume of the binder (cement + glass powder) for mortar made with glass powder
 430 compared to the reference mortar due to the lower bulk density of glass powder (2.5 g/cm^3) compared
 431 to cement (3.16 g/cm^3).

432 From 28 to 90 days, we can see that the porosity reduces and the microstructure becomes more
 433 refined. An increase in the volume of mercury intruded at higher pressure is seen for all mortar made
 434 with glass powder compared to the reference whether at 28 or 90 days, indicating more refined
 435 microstructures. This can be explained by pozzolanic reactions occurring between glass powder and
 436 calcium hydroxide to form more C-S-H gel leading to the refinement and densification of the mortar's
 437 pore structure. These results are in accordance with previous MIP research done by Du et al. [5]. They
 438 studied the effect of glass powder on cement paste and mortar samples collected from the fractured
 439 surfaces of concrete, free of large aggregate particles. Portland cement is replaced at different
 440 contents: 15%, 30%, 45%, and 60% by weight. Their results indicate that glass powder pastes have
 441 more refined pores. Results indicate that the total porosity only marginally varies, and the pore size
 442 distribution is more refined, with increasing GP content.

443 The cumulative intrusion-versus-pore diameter curves for 25 GP GR and 35 GP GR are very close
 444 especially at higher pressures. In addition, total porosity is the same at the same age, 28 and 90 days.
 445 This is consistent with compressive strength results and water porosity results.

Mixture	Porosity (%)		Critical pore diameter (nm)	
	28 Days	90 Days	28 Days	90 Days
0 SCM	11.22	10.74	39.99	41.75
10 GP GR	12.04	11.67	36.91	34.21
25 GP GR	13.60	13.08	39.44	37.79
35 GP GR	13.63	13.26	42.30	43.84
60 GP GR	15.96	15.58	62.98	37.84

446 **Table 5** Critical pore size and total porosity of mortar made with different glass powder content.

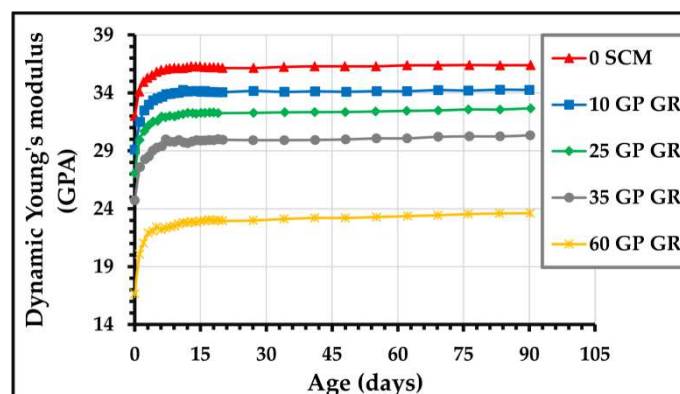
447 Critical pore size corresponding to the steepest slope of the cumulative intrusion curves and total
448 porosity corresponding to the maximum volume intruded are shown in [Tab. 5](#) for 28 and 90 days. At
449 28 days, the critical pore size remains constant for mortar with glass powder or changes slightly
450 compared to the reference, except for the 60 GP GR where the critical pore size increases due to the
451 dilution effect. From 28 to 90 days, the critical pore size marginally changes for all mortars made with
452 glass powder except 60 GP GR where the critical pore size significantly decreases. As said before, the
453 dilution effect leads to bigger pores with 60 GP GR. However, pozzolanic reactions that occur
454 between 28 and 90 days lead to much more refinement of the mortar pore structure. According to Du
455 et al. [5], concrete made with 60% replacement of cement by glass powder shows higher volume
456 fraction of pores in the range of 0.1 μm to 10 μm at 91 days due to insufficient calcium hydroxide
457 reacting with glass powder to further fill the pores.

458 3.6. Dynamic Young's and shear moduli of mortar

459 Dynamic Young's and shear moduli are determined using impulse excitation by vibration. Results
460 shown in [Fig.10](#) and [Fig.11](#) indicate that Dynamic Young's and shear moduli increase with age from
461 the time of demolding until 12 days. After that age, i.e. from 13 days to 90 days, all mortar seems to
462 show stable values of dynamic Young's and shear moduli or indicate very small increases.

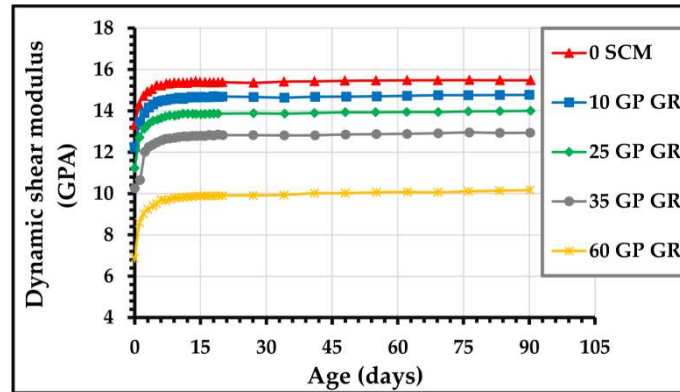
463 [Fig.10](#) shows also that increasing GP content in mortar reduces the dynamic Young's modulus. A
464 significant decrease is seen for 60 GP GR mortar. The same trend is shown in [Fig.11](#) for dynamic
465 shear modulus.

466



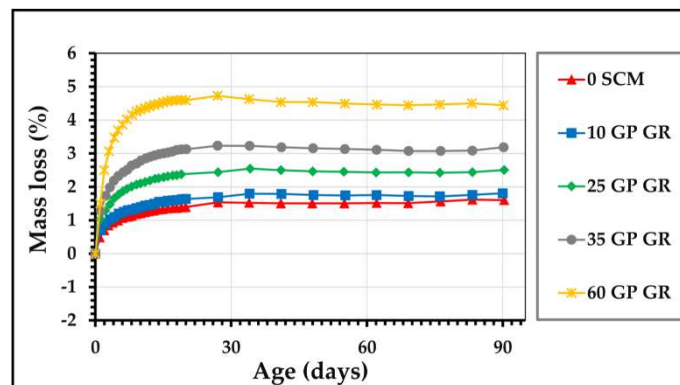
467

468 **Fig. 10.** Dynamic Young's modulus of mortar made with different rates of glass from the time of
469 demolding to 90 days.



470
471 **Fig. 11.** Dynamic shear modulus of mortar made with different rates of glass powder from the time of
472 demolding to 90 days.

473 Fig. 12 shows the weight loss of different mortars from the time of demolding to 90 days.
474 Results from Fig.12 indicate that weight loss increases with increasing glass powder content. Very
475 slight variation in weight loss can be seen for mortar made with 10% glass powder compared to the
476 control mortar. A considerable part of the weight loss occurs before seven days for all mortar studied.
477 After 27 days very slight variation can be seen on mass loss for the different mortars, which is due to
478 variation in humidity curing conditions.



479
480 **Fig. 12.** Mass loss of mortar made with different content of glass powder from the time of
481 demolding to 90 days.

482 When comparing compressive strength to dynamic Young's and shear moduli results, we note that
483 compressive strength increases from 28 days to 90 days but that the dynamic Young's and shear
484 moduli show very little variation. This can be explained by the probability of microcracks

485 development on mortar structure, that slows down the increase in the dynamic Young's and shear
486 moduli with time. The microcracks existence is most likely due to the water lowering caused by
487 evaporation at early age and by consumption during the hydration process including pozzolanic
488 reaction that lead to microstructure refinement. The evaporation of free water from pore capillaries
489 leads to shrinkage due to capillary tension. This turn leads to the apparition of microcracks [50]. As
490 shown by mercury intrusion porosimetry, the hydration process from 28 to 90 days led to the
491 refinement of mortar structures. According to Baroghel-Bouny [51], the hydration processes induces a
492 liquid water content decrease in cementitious materials while the microstructure is hardening and the
493 pore structure is refining. It is well known that capillary tension is inversely proportional to pore
494 radius. Hence, the probability of microcracks appearing is higher with increasing glass powder content
495 because the increased content leads to the refinement of the pores by pozzolanic reactions.

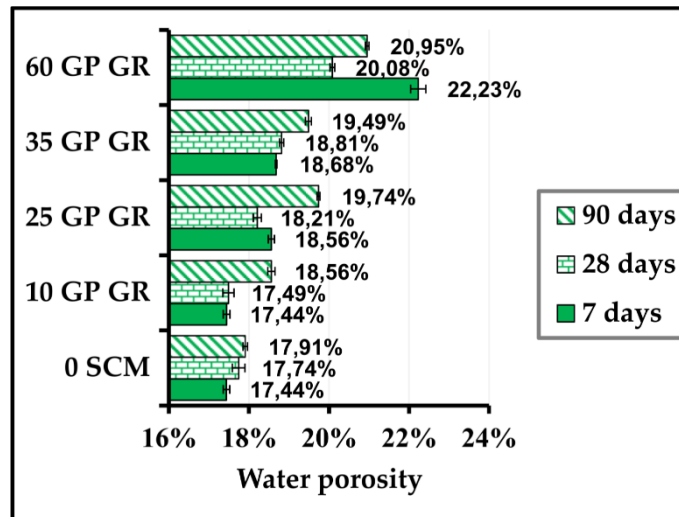
496 **3.7. Water porosity**

497 Fig.13 shows the evolution of the pores accessible to water for mortar samples after 7, 28 and 90 days
498 of curing in water at 20 °C.

499 It can be clearly seen from this figure that the control mortar is less porous than the mortars containing
500 glass powder.

501 The water-accessible porosity of a cementitious material is influenced by its constituents, the
502 hydration process that leads to the formation and change of the microstructure, and testing conditions
503 (vacuum pressure and drying at 105 ° C). The replacement of cement by glass powder increases the
504 water porosity due to the dilution effect. There are less cement and glass particles and much more
505 water in the matrix. The drying effect causes water departure and makes the mortar more porous.
506 Moreover, glass powder has a lower specific gravity than cement and the replacement by mass lead to
507 much more volume of paste (water + cement + glass) in the mortar.

508



509

510 **Fig. 13.** Water accessible porosity of mortar with different glass powder contents at 7, 28 and 90 days.

511 We can see from Fig. 13 that at 7 and 28 days with 10% cement replacement by glass powder, the
 512 porosity remains stable compared to the reference mortar at the same curing ages. By increasing the
 513 rate of cement replacement with glass powder, the water porosity increases for all curing periods,
 514 reaching the highest value at 60% replacement.

515 The water porosity doesn't show great change between 7 and 28 days except the mortar with 60%
 516 replacement. During the hydration process between 7 and 28 days, the hydrates fill parts of the voids
 517 caused by the dilution effect, especially for 60 GP GR, and the porosity decreases slightly.

518 During water porosity testing, samples are exposed to vacuum pressures to evacuate void space. As
 519 said previously, the evaporation of free water can lead to microcracking, especially with high glass
 520 content.

521 Between 28 days and 90 days, all mortars with glass powder show slight increases in water porosity.
 522 This can be explained by the pozzolanic reaction, which occurs; leading to an increase in C-S-H gel in
 523 the matrix and the refinement of the microstructure. The change occurring in water porosity is an
 524 effect of several parameters: filling the void, caused by the dilution effect with newly formed hydrates,
 525 pozzolanic reactions that lead to the refinements of the microstructure and the test conditions (vacuum
 526 pressure and heating at 105°C).

527 When comparing water porosity and mercury porosity values for the same mixture and the same
 528 hydration's age, it is clear that water porosity is higher than mercury porosity. It is well known that

529 mercury porosity qualifies restricted range of the pores structure (from 200 μm to 3 nm in our case),
530 however water can cover large game of porosity than mercury. Moreover, mercury intrusion porosity
531 is determined on sample dried at 40°C and water porosity is calculated based on sample dried at
532 105°C.

533 **4. Conclusions**

534 Waste glass powder from green glass bottles has been investigated for use as cement replacement on
535 cement paste and mortar. The main conclusions that can be taken out from the present work are the
536 following:

537 -The flow of mortars made with glass powder is influenced by several counteracting effects:

- 538 • The nonabsorbent nature of glass particles that increase the effective water to cement (w/c)
539 ratio and enhances the flowability.
- 540 • The irregular shape of particles with high aspect ratio and sharp edges, which decrease the
541 fluidity.
- 542 • The particle sizes where the shape of finer particles increases fluidity but more water is needed
543 to wet their surface.
- 544 • The smooth surface of glass promotes particle movements and increases fluidity.
- 545 • The decrease of the cement paste in the mix arising from high-level replacement increases
546 particle friction and decreases fluidity.

547 -For a water-to-binder ratio (W/B) of 0.5, increased cement replacement by glass powder decreases the
548 compressive strength of mortar at all curing periods in this study (7, 28 and 90 days). This reduction is
549 mainly due to the dilution effect and the non-absorbent nature of glass powder, which increases the
550 effective water-to-binder ratio. The long-term pozzolanic reactions using glass powder is proven
551 through the change in compressive strength from 7 to 90 days especially for mortar made with 60% of
552 glass powder.

553 -It is evidenced by heat evolution normalized relative to the cement component and chemical
554 shrinkage that increasing glass powder content in cement paste increases the reaction rate. The rate of

555 hydration is increased by the physical presence of glass powder. The time to reach the first heat flow
556 peak decreases with an increase of glass content.

557 -The porosity is reduced and the microstructure became more refined from 28 to 90 days for all
558 mortars. The pore size distribution is affected by the glass powder substitution rate. The mortar
559 containing glass powder shows higher porosity than the reference at 28 and 90 days. The highest value
560 is obtained with 60% replacement. This finding is in accordance with the low compressive strength
561 and high water porosity.

562 -High rate of replacement of cement by glass powder leads to bigger pores due to the dilution effect. In
563 contrast, the pozzolanic reaction that occurs between glass powder and calcium hydroxide leads to an
564 increase in C-S-H gel, which leads to the refinement and densification of the pore structure of mortar
565 made with glass powder.

566 -The change occurring in water porosity is an effect of several parameters: filling the void, caused by
567 the dilution effect with newly formed hydrates, pozzolanic reactions that lead to the refinements of the
568 microstructure and the test conditions (vacuum pressure and heating at 105°C).

569 -The Dynamic Young's modulus increases with age from the time of demolding to 12 days. Between
570 13 and 90 days, the Young's modulus for all mortars seems to be stable or shows a very small
571 increase. This can be explained by the probability of microcracks development on mortar structure,
572 that slows down the increase in the dynamic Young's and shear moduli with time. The microcracks
573 existence is most likely due to the water lowering caused by evaporation at early age and by
574 consumption during the hydration process including pozzolanic reaction that lead to microstructure
575 refinement. The increase of glass content in mortar reduces dynamic Young's modulus. A significant
576 decrease is seen for 60 GP GR. The same trends are shown for dynamic shear modulus.

577 We can see from this study that the presence of high glass content in cementitious materials enhances
578 the rate of hydration. This is evidenced by chemical shrinkage and heat assessment. Due to the dilution
579 effect and the nonabsorbent nature of glass, high glass content mortar increases mass loss and
580 porosity. However, pozzolanic reactions increase the refinement of the pore structure. Results also
581 show a significant decrease in the dynamic Young's and shear moduli of mortar made with high glass
582 content.

583 Taking into account economic consideration of using waste glass and the characteristics studied in the
584 present paper, we conclude that 35% cement replacement by green glass powder, can be considered as
585 the optimum for mortar uses. The use of high glass powder content as cement replacement is possible
586 for a water-to-binder ratio of 0.5. It is important to note that further studies related to durability
587 characteristics are needed especially for high glass content on using such mortar as construction
588 materials. It is also recommended to reduce the water-to-binder ratio, which is expected to enhance the
589 durability characteristics of cementitious materials made with green glass powder.

590

591 **5. Reference**

592 [1] R. Idir, M. Cyr, A. Tagnit-Hamou. Pozzolanic properties of fine and coarse color-mixed glass
593 cullet. *Cem. Concr. Compos.* 2011; 33: 19-29.

594 [2] Y. Jiang, T. Ling, K. H. Mo, C. Shi. A critical review of waste glass powder-Multiple roles of
595 utilization in cement-based materials and construction products. *J. Envir. Manag.* 2019; 242: 440-449.

596 [3] J. Harder. Potential Glass recycling - Current market trends. *Recovery-worldwide recycling*
597 *technologies*, Issue 05/2018, [https://www.recovery-worldwide.com/en/artikel/glass-recycling-current-](https://www.recovery-worldwide.com/en/artikel/glass-recycling-current-market-trends_3248774.html)
598 [market-trends_3248774.html](https://www.recovery-worldwide.com/en/artikel/glass-recycling-current-market-trends_3248774.html).

599 [4] J. Barton, C. Guillemet. *Science and technology glass*. EDP sciences 2005; 464 P. ISBN 2-86883-
600 789-1.

601 [5] H. Du, K. H. Tan. Properties of high volume glass powder in concrete. *Cem. Concr. Compos.*
602 2017; 75: 22-29.

603 [6] M. C. Bignozzi, A. Saccani, L. Barbieri, I. Lancellotti. Glass waste as supplementary cementing
604 materials: The effects of glass chemical composition. *Cem. Concr. Compos.* 2015; 55: 45-52.

605 [7] W. Jin, C. Meyer, S. Baxter. "Glascrete"-Concrete with Glass. *ACI Mat. J.*2000; Title no. 97- M
606 27.

- 607 [8] A. Schmidt, W. H. F. Saia. Alkali-aggregate reaction tests on glass used for exposed aggregate
608 wall panel work." *ACI Mat. J.* 1963; 60: 1235-1236.
- 609 [9] C. Polley, S. M. Cramer, RV. de la Cruz. Potential for using waste glass in Portland cement
610 concrete. *J. Mater. Civil. Eng.* 1998; 10: 210-9.
- 611 [10] ÍB. Topçu, AR. Bagã, T. Bilir. Alkali-silica reactions of mortars produced by using waste glass as
612 fire aggregate and admixtures such as fly ash and Li_2CO_3 . *Waste. Manag.* 2008; 28 (5): 878-84.
- 613 [11] H. Du, K. H. Tan. Use of waste glass as sand in mortar: Part II - Alkali-silica reaction and
614 mitigation methods. *Cem. Concr. Compos.* 2013; 35 (1): 118-126.
- 615 [12] T. C. Ling, C. S. Poon. Feasible use of large volumes of GGBS in 100% recycled glass
616 architectural mortar. *Cem. Concr. Compos.* 2014; 53: 350–356.
- 617 [13] R. Idir, M. Cyr, A. Tagnit-Hamou. Use of fine glass as ASR inhibitor in glass aggregate mortars.
618 *Constr. Build. Mater.* 2010; 24: 1309-1312.
- 619 [14] A. Shayan, A. Xu. Value-added utilisation of waste glass in concrete. *Cem. Concr. Res.* 2004; 34
620 (1): 81-89.
- 621 [15] M. Carsana, M. Frassoni, L. Bertolini. Comparison of ground waste glass with other
622 supplementary cementitious materials. *Cem. Concr. Compos.* 2014; 45: 39-45.
- 623
624 [16] M. Liu. Incorporating ground glass in self-compacting concrete. *Constr. Build. Mater.* 2011; 25:
625 919-925.
- 626 [17] Y. Shao, T. Lefort, S. Moras, D. Rodriguez, Studies on concrete containing ground waste glass.
627 *Cem. Concr. Res.* 2000; 30: 91-100.
- 628 [18] CSA-A3000-18 standard. Cementitious materials compendium. Canadian Standards Association
629 2018. ISBN 978-1-4883-1323-3.

- 630 [19] M. Mirzahosseini, K. A. Riding. Influence of different particle sizes on reactivity of finely ground
631 glass as supplementary cementitious material (SCM). *Cem. Concr. Compos.* 2015; 56: 95-105.
- 632 [20] D. Patel, R. P. Tiwari, R. Shrivastava, R. K. Yadav. Effective utilization of waste glass powder as
633 the substitution of cement in making paste and mortar. *Constr. Build. Mater.* 2019; 199: 406-415.
- 634 [21] A. A. Aliabdo, A. E.M. Abd Elmoaty, A.Y. Aboshama. Utilization of waste glass powder in the
635 production of cement and concrete. *Constr. Build. Mater.* 2016; 124: 866-877.
- 636 [22] A. Parghi, M. Shahria Alam. Physical and mechanical properties of cementitious composites
637 containing recycled glass powder (RGP) and styrene butadiene rubber (SBR). *Constr. Build. Mater.*
638 2016; 104: 34-43.
- 639 [23] L. A. Pereira-de-Oliveira, J. P. Castro-Gomes, P. M. S. Santos. The potential pozzolanic activity
640 of glass and red-clay ceramic waste as cement mortars components. *Constr. Build. Mater.* 2012; 31:
641 197-203.
- 642 [24] C. Shi, Y. Wu, C. Riefler, H. Wang. Characteristics and pozzolanic reactivity of glass powders.
643 *Cem. Concr. Res.* 2005; 35: 987- 993.
- 644 [25] H. Du, K. H. Tan. Transport properties of concrete with glass powder as supplementary. *ACI*
645 *Mat. J.* 2015; 112 (3).
- 646 [26] N. Neithalalath. Quantifying the effects of hydration enhancements and dilutions enhancements in
647 cements pastes containing coarse glass powder. *J. Adv. Concr. Tech.* 2008; 6: 397-408.
- 648 [27] H. Du, K. H. Tan. Waste glass powder as cement replacement in concrete cementitious materials
649 compendium 2014. *J. Adv. Concr. Tech.* 12: 468-477.
- 650 [28] G. Liu, M.V.A. Florea, H. J. H. Brouwers. Performance evaluation of sustainable high strength
651 mortars incorporating high volume waste glass as binder. *Constr. Build. Mater.* 2019; 202: 574-588.
- 652 [29] EN 196-1. Methods of testing cement- Part 1: Determination of strength. European committee for
653 standardization, 2006.
- 654 [30] EN 197-1. Cement - Part 1: Composition, specifications and conformity criteria for common
655 cements. European committee for standardization 2000.

656 [31] EN 1015-3. Methods of test for mortar for masonry-Part 3: Determination of consistence of fresh
657 mortar. European committee for standardization 1999.

658 [32] W. Deboucha, N. Leklou, A. Khelidj, M. N. Oudjit. Hydration development of mineral additives
659 blended cement using thermogravimetric analysis (TGA): Methodology of calculating the degree of
660 hydration. *Constr. Build. Mater.* 2017; 146: 687-701.

661 [33] G. D. Moon, S. Oh, Y. C. Choi. Effects of the physicochemical properties of fly ash on the
662 compressive strength of high-volume fly ash mortar. *Constr. Build. Mater.* 2016; 1072-1080.

663 [34] P. Mounanga, A. Khelidj, A. Loukili, V. Baroghel Bouny. Predicting Ca (OH)₂ content and
664 chemical shrinkage of hydrating cement pastes using analytical approach. *Cem. Concr. Res.* 2004; 34:
665 255-265.

666 [35] M. Bouasker, P. Mounanga, P. Turcry, A. Loukili, A. Khelidj. Chemical shrinkage of cement
667 pastes and mortars at very early age: effect of limestone filler and granular inclusions. *Cem. Concr.*
668 *Compos.* 2008; 30 (1): 13-22.

669 [36] H. Giesche. Mercury porosimetry: A General (practical) overview. *Part. Part. Syst. Charact* 2006;
670 23: 9-19. DOI: 10.1002/ppsc.200601009

671 [37] S. Diamond. Mercury porosimetry. An inappropriate method for the measurement of pore size
672 distributions in cement-based materials. *Cem. Concr. Res.* 2000; 30: 1517-1525.

673 [38] ASTM E 1876-01. Standard Test Method for Dynamic Young's Modulus, Shear Modulus, and
674 Poisson's Ratio by Impulse Excitation of Vibration 1. *Mater. Scien.* 2005.

675 [39] NF EN ISO 12680-1. Méthodes d'essai pour produits réfractaires - Partie 1 : détermination du
676 module de Young dynamique (MOE) par excitation de vibration par impulsion. French Association
677 for Standardization 2007.

678 [40] NF P 18-459. Concrete - Testing Hardened Concrete-Testing Porosity and Density.
679 French Association for Standardization AFNOR 2010.

680 [41] G. M. Sadiqul Islam, M. H. Rahman, N. Kazi. Waste glass powder as partial replacement of
681 cement for sustainable concrete practice. *Inter. J. Sustain. Buil. Envir.* 2016; 6: 37-44.

- 682 [42] B. Taha, G. Nounu. Properties of concrete contains mixed colour waste recycled glass as sand and
683 cement replacement. *Constr. Build. Mater.* 2008; 22: 713-720.
- 684 [43] N. Schwarz, M. DuBois, N. Neithalath. Electrical conductivity based characterization of plain and
685 coarse glass powder modified cement pastes. *Cem. Concr. Compos.* 2007; 29: 656-666.
- 686 [44] J. Lu, Z. Duan, C. S. Poon. Fresh properties of cement pastes or mortars incorporating waste glass
687 powder and cullet. *Constr. Build. Mater.* 2017; 131: 793-799.
- 688 [45] L. Huang, P. Yan. Effect of alkali content in cement on its hydration kinetics and mechanical
689 properties. *Constr. Build. Mater.* 2019; 228: 116833.
- 690 [46] A. Khmiri, M. Chaabouni, B. Samet. Chemical behaviour of ground waste glass when used as
691 partial cement replacement in mortars. *Constr. Build. Mater.* 2013; 44: 74-80.
- 692 [47] I. Jawed, J. Skalny. Alkalies in cement: A review II. Effects of alkalies on hydration and
693 performance of Portland cement. *Cem. Concr. Res.* 1978 ; 8: 37-52.
- 694 [48] K. L. Scrivener, P. Juilland, P. J. M. Monteiro. Advances in understanding hydration of Portland
695 cement. *Cem. Concr. Res.* 2015; 78: 38-56.
- 696 [49] W. Yodsudjai, K. Wang. Chemical shrinkage behaviour of pastes made with different types of
697 cements. *Constr. Build. Mater.* 2013; 40: 854-862.
- 698 [50] A. Khelidj, A. Loukili, G. Bastian. Experimental study of the hydro-chemical coupling inside
699 maturing concretes: effect on various types of shrinkage. 1998; 31: 588-594.
- 700 [51] V. Baroghel-Bouny, M. Mainguy, T. Lassabatere, O. Coussy. Characterization and identification
701 of equilibrium and transfer moisture properties for ordinary and high-performance cementitious
702 materials. *Cem. Concr. Res.* 1999; 29:1225–1238.